Quantum Nano-Electronics

Hervé Courtois

Institut Néel
CNRS, Université Joseph Fourier and Grenoble INP

http://neel.cnrs.fr/spip.php?article804&lang=en
herve.courtois@neel.cnrs.fr

Part 3:
Quantum transport

Chapter 1:
General concepts

Characteristic length scales

Electron wavelength λ_F < 1 nm for metals:

$$E_F = \frac{\left[\hbar k_F\right]^2}{2m} = \frac{\left[\hbar/\lambda_F\right]^2}{2m} \qquad \lambda_F = \frac{\hbar}{\sqrt{2mE_F}}$$

Electron elastic mean free path in a diffusive metal: l_e = 10-100 nm

Phase coherence length: L_φ = 1-10 µm at low temperature

Inelastic scattering length: $L_{in} \geqq L_\varphi$ = 1-10 µm at low temperature

Sample size: L = 10 nm – 10 µm

Mesoscopic, microscopic, macroscopic

Macroscopic: usually considered in the thermodynamic limit $N \to \infty, V \to \infty$

Microscopic: discrete spectrum of energy levels, concept of impurity ensemble breaks down, discreteness of electric charge and magnetic flux, ballistic transport, coherent motion of electrons.

Mesoscopic: system size is intermediate, small enough so that phase coherence is preserved.
Example: a 1 μm^2 x 30 nm metal island has about 10 billions electrons, but removing one makes a difference.

The Thouless energy

Sample length: $L = \sqrt{D\tau}$
Time taken to travel: $\tau = \frac{L^2}{D}$

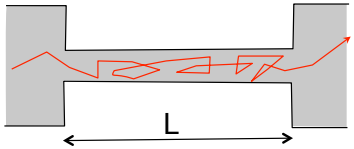

Related energy through uncertainty relation:

$$E_{Th} = \frac{\hbar D}{L^2}$$

Macroscopic regime: $E_{Th} < k_B T$ $\quad L > L_T = \sqrt{\frac{\hbar D}{2\pi k_B T}}$
Mesocopic regime: $E_{Th} > k_B T$:
If l_e = 30 nm in Cu, D = 150 cm^2/s, L_T = 0.2 μm at 1 K, E_{th} = 4 μeV for L = 1 μm.

Meaning of Thouless energy:
Phase acquired during diffusion through the sample = $E.\tau/\hbar$
If energy varies by E_{Th}, phase changes by 2π.

A mesoscopic sample

A phase-coherent conductor of any kind:
metal, nanotube, molecule, graphene, 2DEG …

Connected to reservoirs with a well-defined chemical potential.
They are source of electrons at thermal equilibrium energy distribution.
Dissipation occurs in the reservoirs.

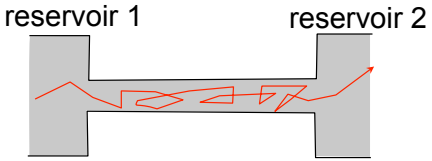

In practice a rather massive (wide and/or thick) electrode is enough.

Out-of-equilibrium energy distribution

A superconducting tunnel junction used for energy distribution spectroscopy.
Sample is normal, probe is superconducting:

$$I \propto \int_{-\infty}^{+\infty} N_{probe}(E)\left[f_{probe}(E - eV) - f_{sample}(E)\right]dE$$

N_{probe} calibrated at zero bias, f_{probe} known.
f_{sample} is extracted from measured I(V).

A sharp DOS is needed for an accurate determination.

H. Pothier et al, Phys. Rev. Lett. 79, 3490 (1997).

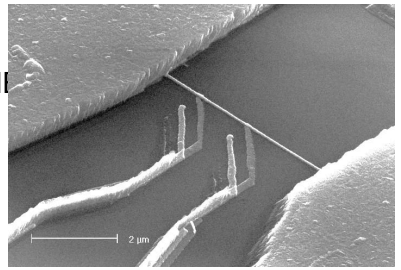

FIG. 1. Experimental layout: a metallic wire of length L is connected at its ends to reservoir electrodes, biased at potentials 0 and U. In the absence of interaction, the distribution function at a distance $X = xL$ from the grounded electrode has an intermediate step $f(E) = 1 - x$ for energies between $-eU$ and 0 (solid curves) (we assume $U > 0$). When interactions are strong enough to thermalize electrons, the distribution function is a Fermi function, with a space-dependent temperature and electrochemical potential (dotted curves). In the experiment, the distribution function is obtained from the differential conductance $dI/dV(V)$ of the tunnel junction formed by the wire and a superconducting electrode placed underneath.

Out-of-equilibrium energy distribution

Double step distribution function = a linear combination of the two reservoirs' distributions.

Smearing due to e-e interactions:
Inelastic scattering tends to a local quasi-equilibrium.

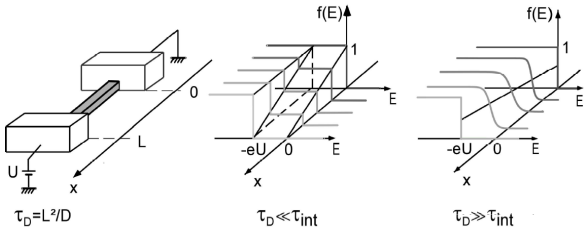

A. Anthore thesis.

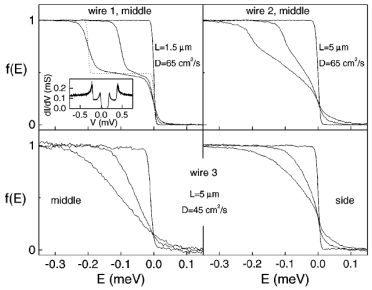

FIG. 2. Inset of the top left panel: Measured $dI/dV(V)$ of the tunnel junction to wire 1 for $U = 0.2$ mV. In the four panels, distribution functions, obtained from the deconvolution of such $dI/dV(V)$ curves, for $U = 0$, 0.1, and 0.2 mV in the middle of a 1.5-μm-long wire with a diffusion constant $D \sim 65$ cm^2/s (wire 1, top left); in the middle of a 5-μm-long wire with the same diffusion constant (wire 2, top right); in the middle (bottom left) and at 1.1 μm from the grounded reservoir electrode (bottom right) of a 5-μm-long wire (wire 3) with $D \sim 45$ cm^2/s. Also plotted as a dotted line in the top left panel is the prediction for the noninteracting distribution function [Eq. (2)] for $U = 0.2$ mV. All measurements were performed at 25 mK. The cross-sectional area of the three wires is nominally the same: 45×110 nm^2. The tunnel resistances of the junctions were $R_T = 10$ kΩ for wires 1 and 2, $R_T = 200$ kΩ for the middle junction on wire 3, and $R_T = 75$ kΩ for the side junction on wire 3.

Hot-electron regime

Wiedemann-Franz law between electrical and thermal conductivities: $\frac{\kappa}{\sigma} = \mathcal{L}T$

where $\mathcal{L}$ is the Lorentz number. $\mathcal{L} = \frac{\pi^2}{3}\frac{k_B^2}{e^2}$

Assume local equilibrium: $\frac{d}{dX}\left(\kappa\frac{dT}{dX}\right)dX = \frac{d}{dX}\left(\frac{L}{R}\mathcal{L}T\frac{dT}{dX}\right)dX = \frac{U^2}{R}\frac{dX}{L}$

$$\frac{d^2T^2}{dX^2} = \frac{2U^2}{\mathcal{L}L^2}$$

Solution: $T_{eff}(x) = \sqrt{T_{bath}^2 + x(1-x)U^2/\mathcal{L}}$ $\quad x = \frac{X}{L}$

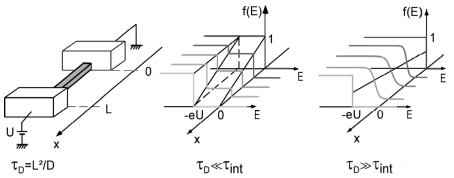

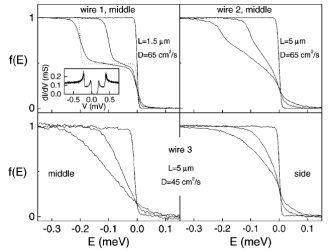

1.2: The conductance quantization

Electrons as fermions

Pauli principle: a state is occupied by one electron or empty.

Density of states in k space in 3D $\frac{2}{(2\pi)^3}$

Energy distribution function f determined by statistics.

Expression for the current density: $J = \int 2\frac{d^3k}{(2\pi)^3} e.v(k).f(k)$

Electrons as plane waves

In vacuum: $\Psi(\vec{r},t) = \frac{1}{\sqrt{V}}\exp\left(i\vec{k}.\vec{r} - \frac{i}{\hbar}E(k)t\right)$

In a ballistic conductor as a wave-guide:
1D free motion (x) + confinement in y,z directions

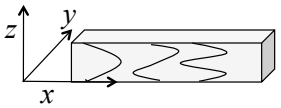

$$\Psi_{k_x,n}(\vec{r},t) = \phi_n(y,z)\exp\left(ik_x.x - \frac{i}{\hbar}Et\right)$$

Energy of the mode n:

$$E = \frac{(\hbar k_x)^2}{2m} + E_n$$

with $E_n = \frac{\pi^2\hbar^2}{2m}\left\{\frac{n_y^2}{a(x)^2} + \frac{n_z^2}{b(x)^2}\right\}$

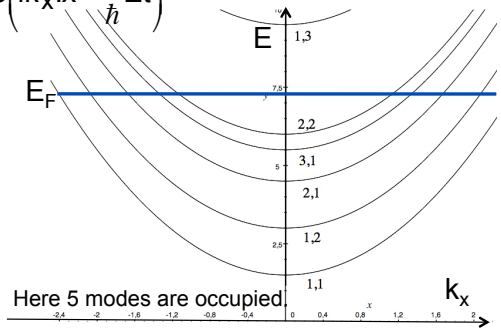

Adiabatic transport

A quantum point contact (QPC) = constriction in the mesoscopic regime:

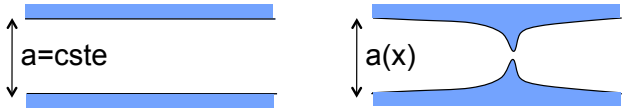

Variation of dimension occurs on a scale large compared to width:
the usual approach can be used locally.

$$E_n = \frac{\pi^2\hbar^2}{2m}\left\{\frac{n_y^2}{a(x)^2} + \frac{n_z^2}{b(x)^2}\right\}$$

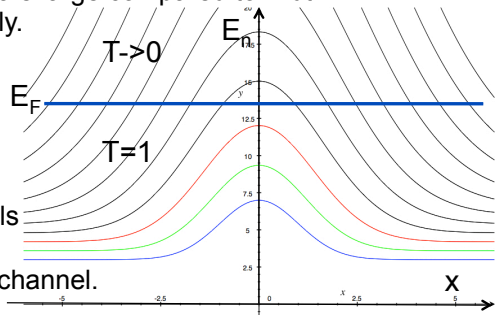

A reduced number (here 3) of channels is fully transmitted.
A transparency T is defined for every channel.

Conductance of a quantum point contact

Net current = current of right-moving particules – current of left-moving ones.

For every channel:

$$J_{\rightarrow} = \frac{2}{2\pi}\int dk_x.e.v_x(k_x).f_{left}(k_x)$$

$$J_{\leftarrow} = \frac{2}{2\pi}\int dk_x.e.v_x(k_x).f_{right}(k_x)$$

We have:

$$v_x = \frac{1}{\hbar}\frac{\partial E}{\partial k_x}$$

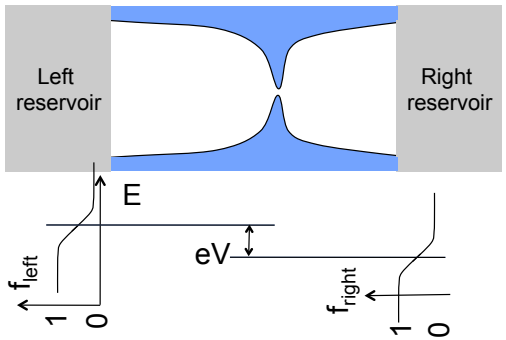

Let's consider that a limited number of channels is open: T=1.

$$I = \frac{2e}{2\pi\hbar}\sum_{channels}\int dE.\left[f_{left}(E) - f_{right}(E)\right] = 2\frac{e^2}{h}N_{open}V$$

Conductance of a quantum point contact

One obtains: $I = 2\frac{e^2}{h}N_{open}V = 2G_Q V$

The conductance is quantized: $G = 2N_{open}G_Q$

Factor 2 due to spin.

The conductance quantum G_Q is $\frac{1}{25.8\,k\Omega}$.

The conductance is relevant here, not conductivity nor resistance or resistivity.
The conductance is finite even if the channel is ballistic: contact resistance.

Conductance quantization: experiment

Two-dimensionnal electron gas (2DEG) made from a GaAs-AlGaAs heterostructure. A negative bias on a top gate depletes the gas.
First demonstration of conductance quantization:

B. J. van Wees et al, Phys. Rev. Lett. 60, 848 (1988).

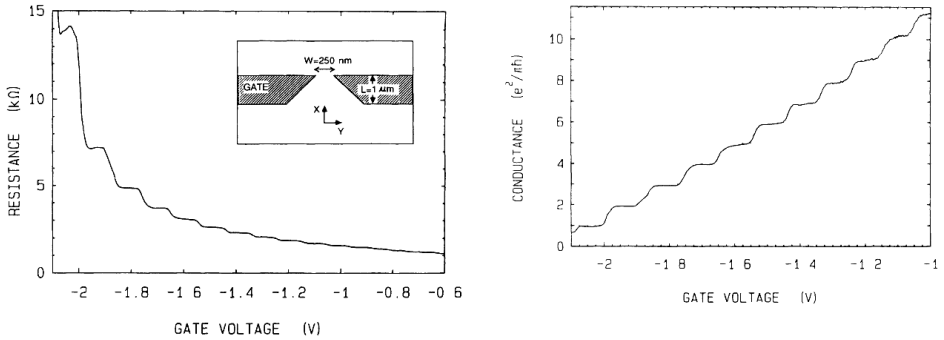

1.3: Landauer formalism

Conductance of a coherent conductor

Up to now, modes are either transmitted or reflected.

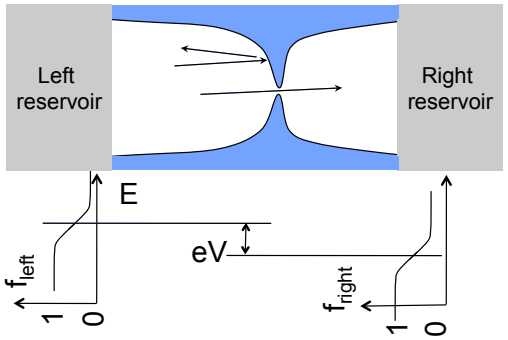

Conductance of a coherent conductor

Some modes can be partially transmitted.
A conduction channel can be partially transmitted: $0 \leq T \leq 1$.

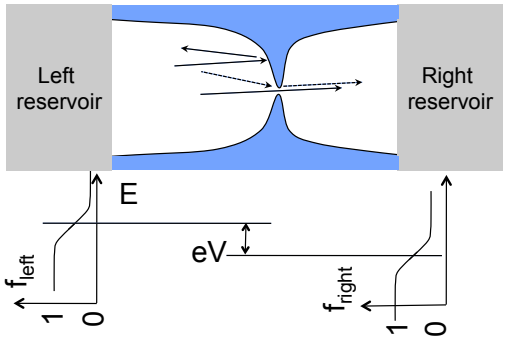

Conductance quantization : experiment

As a simple approach (not a demonstration), let us add a transmission:

$$I = \frac{2e}{2\pi\hbar}\sum_p \int dE.T_p(E).\left[f_{left}(E) - f_{right}(E)\right] = 2G_Q \sum_p T_p V$$

Landauer-Bütiiker formula: $G = \sum_p 2\frac{e^2}{h} T_p = 2G_Q \sum_p T_p$

A full demonstration includes a transmission matrix t.
The channels p considered above are then eigenstates of $t^\dagger t$.

Restriction: only elastic processes are considered. No e-e interactions.
Implies: low T, small dimensions, low voltage.

Visualization of the conductance channels

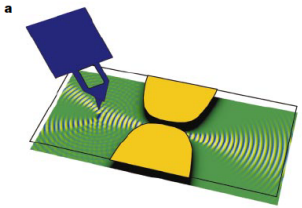

Scanning gate microscopy (SGM):

A tip is used as a local gate that depletes locally a 2DEG.

The resistance change measures the local density of current.

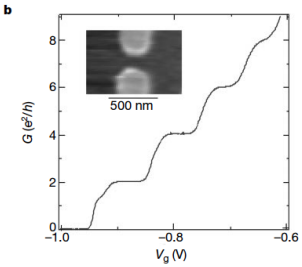

Figure 1 Experimental set-up. **a**, Schematic diagram of the experimental set-up used for imaging electron flow. The tip introduces a movable depletion region which scatters electron waves flowing from the quantum point contact (QPC). An image of electron flow is obtained by measuring the effect the tip has on QPC conductance as a function of tip position. Two ohmic contacts ~1 mm away from the QPC (not shown) allow the conductance of the QPC to be measured using an a.c. lock-in amplifier at 11 kHz. The root-mean-square voltage across the QPC, 0.2 mV, was chosen in order not to heat electrons significantly above the lattice temperature of 1.7 K. **b**, Conductance of the QPC used for Fig. 2b versus QPC width controlled by the gate voltage. Steps at integer multiples of $2e^2/h$ are clearly visible. The inset is a topographic AFM image of the QPC.

M. A. Topinka et al, Nature 410, 183 (2001).

Visualization of the conductance channels

Individual conductance channels are observed.

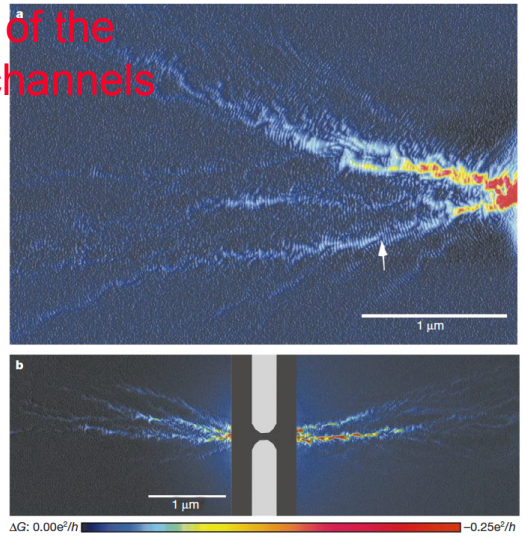

Figure 2 Experimental images of electron flow. **a**, Image of electron flow from one side of a QPC at $T = 1.7$ K, biased on the $G = 2e^2/h$ conductance step. Dark regions correspond to areas where the tip had little effect on QPC conductance, and hence are areas of low electron flow. The colour varies and the height in the scan increases with increasing electron flow. Narrow branching channels of electron flow are visible, and fringes spaced by $\lambda_F/2$, half the Fermi wavelength, are seen to persist across the entire scan. **b**, Images of electron flow from both sides of a different QPC, again biased on the $G = 2e^2/h$ conductance step. The gated region in the centre was not scanned. Strong channelling and branching are again clearly visible. The white arrow points out one example of the formation of a cusp downstream from a dip in the potential.

Channel transmission in a metallic wire

Conductance chamnnels can be defined in a mesoscopic wire as well.
They are numerous, about 10^5 in a 100x100 nm^2.

Dorotkov distribution of channel transparency.

$$P(T) \propto \frac{1}{T\sqrt{1-T}}$$

Bi-modal distribution with mainly fully open or almost closed channels.

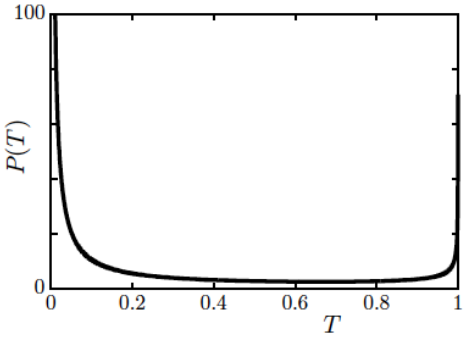

O. N. Dorokhov et al, JETP Lett. 36, 318 (1982).

Chapter 2:
Quantum interference effects

2.1: Universal Conductance Fluctuations

Diffusion probabilities

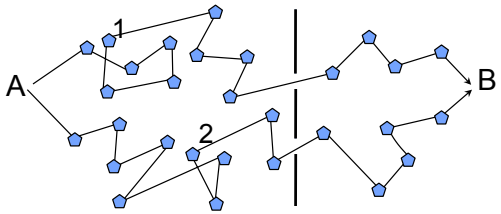

Double-slit experiment: two possible paths from A to B.
Consider the quantum probability $A_{1,2}$ for a particule to move from A to B.

$$P_{A\to B} = |A_1 + A_2|^2 = \underbrace{|A_1|^2}_{=P_1} + \underbrace{|A_2|^2}_{=P_2} + \underbrace{A_1A_2^* + A_1^*A_2}_{=2\mathrm{Re}\left[A_1A_2^*\right]}$$

classical

quantum

Interference

Interference term can be positive or negative.

$$P_{A\to B} = P_{classical} + 2\sqrt{P_1P_2}\cos\delta\phi$$

Electronic wavefunction: $\Psi(x) = \Psi_0 \exp[i\phi(x)] = \Psi_0 \exp[ik(x)x]$

The phase spatial dependence is: $\frac{d\phi}{dx} = k(x) = \sqrt{2m[E - V(x)]}/\hbar$

Phase shift between the two trajectories 1 and 2:

$$\delta\phi_{disorder} = \phi_1 - \phi_2 = \int_1 \vec{k}.d\vec{r} - \int_2 \vec{k}.d\vec{r}$$

$\delta\phi_{disorder}$ is related to the microscopic realization of the disorder:
depends on positions of the scattering centers.
Also on bias and electron density.

Universal Conductance Fluctuations (UCF): experiment

The conductance fluctuates in a reproducible (universal) way, this is not noise.
Magnetic fingerprint of the disorder realization.
Symmetry relationship between measurements with different contact geometry.

$R_{14,23}(B) = R_{23,14}(-B)$

Fluctuations appear with amplitude of about G_Q: at most a one-channel contribution is visible.

A. Benoit et al, Phys. Rev. Lett. 57, 1765 (1986).

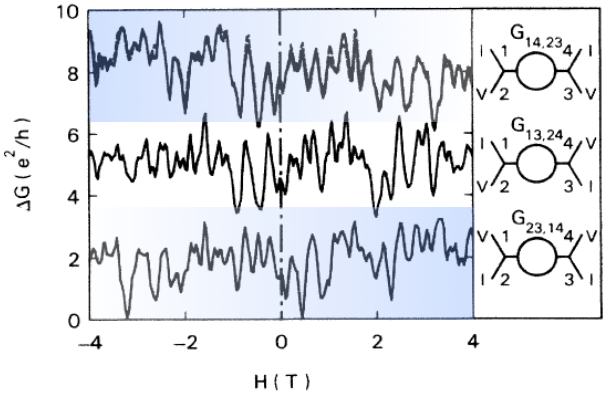

2.2: Aharonov-Bohm effect

Aharonov-Bohm effect

Interference in multiply-connected conductors, like a ring.
A magnetic field creates a vector potential A.

Phases to be calculated with $\vec{k} \to \vec{k} + \frac{e}{\hbar}\vec{A}(x)$

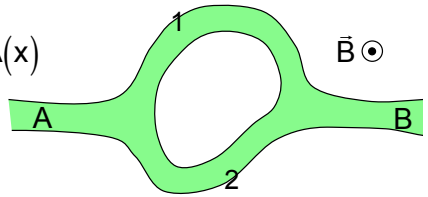

$$\phi_{1,2} = \int_{1,2}\left[\vec{k} + \frac{e}{\hbar}\vec{A}\right]d\vec{r} = \int_{1,2}\vec{k}d\vec{r} + \frac{e}{\hbar}\int_{1,2}\vec{A}.d\vec{r}$$

$$\delta\phi = \phi_1 - \phi_2 = \delta\phi_{disorder} + \frac{e}{\hbar}\oint\vec{A}.d\vec{r} = \delta\phi_{disorder} + \frac{e}{\hbar}\iint_S\vec{B}.\overrightarrow{dS}$$

Phase difference related to flux in the loop, even with no flux in the conductor.

$$\delta\phi = \delta\phi_{disorder} + \frac{e}{\hbar}\Phi = \delta\phi_{disorder} + 2\pi\frac{\Phi}{\Phi_0}$$

$$\Phi_0 = \frac{h}{e}$$

Flux quantum (e instead of 2e for a sc)

Aharonov-Bohm effect

Contributions from every conduction channel add with random phases.

Oscillations appear with period h/e and amplitude of about G_Q: at most a one-channel contribution is visible.

R. A. Webb et al, Phys. Rev. Lett. 54, 2696 (1985).

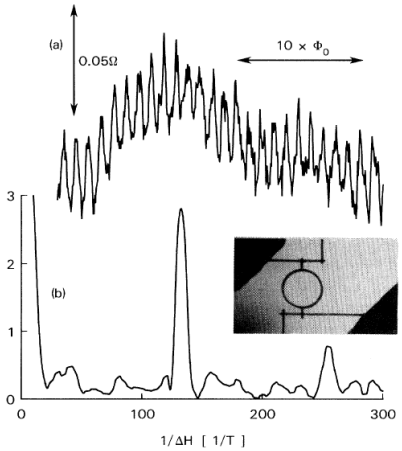

2.3: Weak localization

Weak localization

Consider many different paths from A to B.

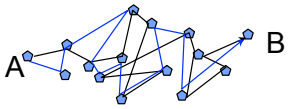

Average = long wire compared to L_φ

$$P_{A\to B} = P_{classical} + 2\sqrt{P_1 P_2}\cos\delta\phi \qquad \langle\cos\delta\varphi\rangle = 0$$

$$\delta\phi_{disorder} = \phi_1 - \phi_2 = \int_1 \vec{k}.d\vec{r} - \int_2 \vec{k}.d\vec{r} = kL_1 - kL_2$$

Phase ϕ is random: most contributions average out.

Consider special trajectories: from A to A, through B.
In zero field, there is no phase difference:

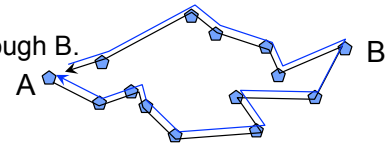

$$\delta\phi_{disorder} = \phi_1 - \phi_2 = 0$$

$$A_2 = A_1$$

$$P_{A\to B} = \left|A_1 + A_2\right|^2 = \left|A_1 + A_1\right|^2 = 4\left|A_1\right|^2$$

Amplitude of backscattering multiplied by 4: localization!

Weak localization

Phase diff. between time-reversed paths, taking into account potential vector.

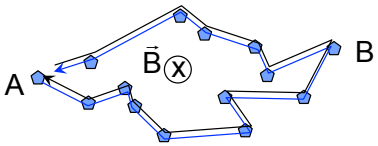

$$\phi_1 - \phi_2 = \frac{2e}{\hbar}\oint \vec{A}.d\vec{r} = \frac{4\pi}{\Phi_0}\iint_S \vec{B}.\overrightarrow{dS} = 4\pi\frac{B.S}{\Phi_0}$$

$$\Phi_0 = \frac{h}{e}$$

S: area enclosed by the flux.
The larger the field, the fewer loops contribute to constructive backscattering.

In a continuous media, the characteristic loop size is: $S \approx L_\varphi^2$

Related characteristic magnetic field: $B_\varphi = \dfrac{\hbar}{2eL_\varphi^2}$

Magnitude of about a conductance quantum.

Weak localization

Coherent backscattering.

Called **weak localization**: small relative number of contributing closed loops.
To be distinguished from strong localization due to strong disorder.

Persists under ensemble average for example in a sample long compared to L_φ.

Resistance expected to increase at small magnetic field.
Decays on the characteristic field B_φ.

Weak localization: experiments

WL magnetoresistance of a metal wire at low temperature:
positive or negative depending on spin-orbit interaction.
Phase coherence time can be deduced.

F. Pierre et al, Phys. Rev. B 68, 085413 (2003).

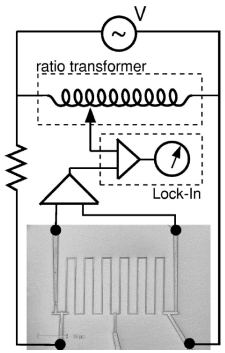

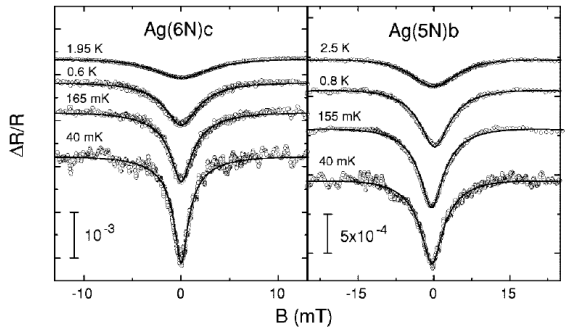

Measurement of a phase coherence time

Phase coherence time limited by:
phonons at intermediate temperature and
e-e interaction at the lowest temperature (α T^{-1}).

τ_φ predicted to diverge at zero temperature.

Low temperature saturation can be observed due to magnetic impurities.

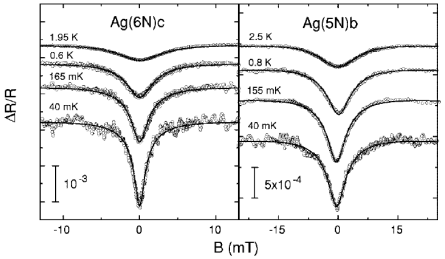

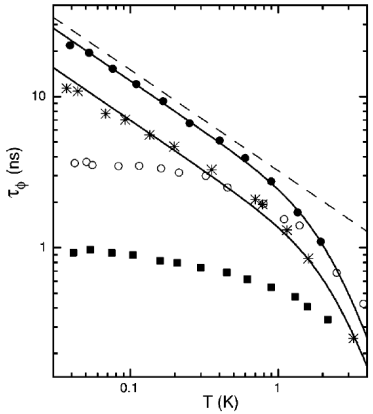

What is needed is a disordered media

Diffusion of light in a water with a suspension of polystirene spheres also shows WL.

P. E. Wolf and G. Maret, Phys. Rev. Lett. 55, 2696 (1985).

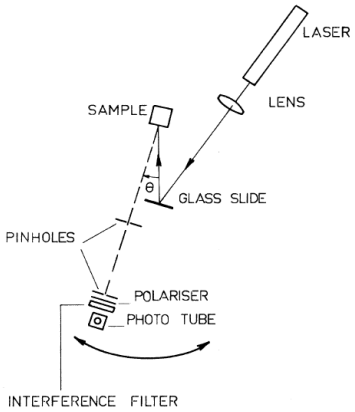

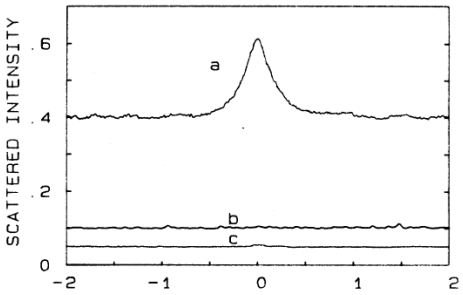

2.4: Aronov-Alshuler-Spivak (AAS) oscillations

Weak localization

Phase diff. between time-reversed paths, taking into account potential vector.

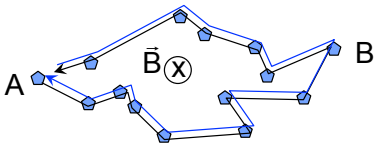

$$\phi_1 - \phi_2 = \frac{2e}{\hbar}\oint \vec{A}.d\vec{r} = \frac{4\pi}{\Phi_0}\iint_S \vec{B}.\overrightarrow{dS} = 4\pi\frac{B.S}{\Phi_0} \qquad \Phi_0 = \frac{h}{e}$$

Period h/2e because two paths instead of one for UCF.

Aronov-Alshuler-Spivak oscillations

In a loop geometry:
Conductance effect of the order of conductance quantum.

$$\Delta G \approx \frac{e^2}{h}$$

Small relative amplitude when conductance large.

$$\Delta R \approx \frac{\Delta G}{G^2} = \frac{e^2}{h}R^2$$

Minimum at zero magnetic field.

B. Pannetier et al, Phys. Rev. B 31, 3209 (1985).

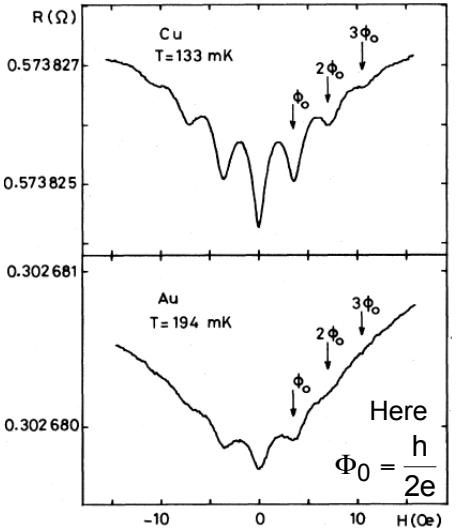

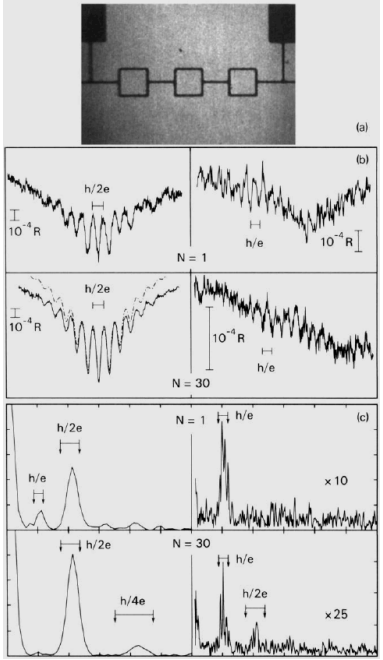

Ensemble average

Add N loops in series: ensemble average.
h/e AB effect vanishes, AAS oscillations survive.

C. Umbach et al, Phys. Rev. Lett. 56, 386 (1986).

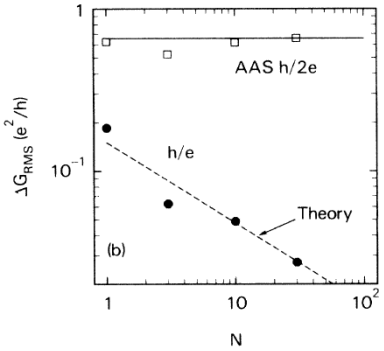

Chapter 3: Persistent currents

Electron states are periodic in flux

Let us consider a single 1D ballistic loop of radius R, with zero potential.

In cylindrical coordinates (r,θ,φ), the Hamiltonian writes:

$$H = \frac{1}{2m}\left[\vec{p} - e\vec{A}\right]^2 = \frac{\hbar^2}{2m}\left[\frac{1}{R}\frac{\partial}{\partial\theta} + \frac{i}{R}\frac{\Phi}{\Phi_0}\right]^2 \qquad \vec{A} = \vec{e}_\theta \frac{\Phi}{2\pi R}$$

Shrödinger eq.: $H\Psi = E\Psi$ $\qquad \psi(\theta + 2\pi) = \psi(\theta)$

Let use a gauge transformation: $$\psi'(\theta) = \psi(\theta)\exp\left(\frac{ie}{\hbar}\int_0^{R\theta}\vec{A}.\vec{dl}\right) = \psi(\theta)\exp\left(i\frac{\Phi}{\Phi_0}\theta\right)$$

Shrödinger equation: $$-\frac{\hbar^2}{2mR^2}\frac{d^2}{d\theta^2}\psi'(\theta) = E\psi'(\theta)$$

equivalent to zero field case -> plane waves.

Solution in a 1D ballistic case

Solutions $\psi'_n(\theta) = \frac{1}{\sqrt{2\pi}}\exp[ix\theta]$ + periodic limit condition:

$$\psi(\theta + 2\pi) = \psi(\theta) \Rightarrow \psi'(\theta + 2\pi) = \psi'(\theta)\exp\left(-2i\pi\frac{\Phi}{\Phi_0}\right)$$

Solutions to the Shrödinger equation are Ψ_n, n is an integer

$$\psi'_n(\theta) = \frac{1}{\sqrt{2\pi}}\exp\left[i\left(n + \frac{\Phi}{\Phi_0}\right)\theta\right]$$

The eigenvalues ε_n are (L=2πR): $H\Psi = E\Psi \Rightarrow \varepsilon_n = \frac{h^2}{2mL^2}\left(n + \frac{\Phi}{\Phi_0}\right)^2$

meaning that the wave-vectors are: $k_n = \frac{2\pi}{L}\left(n + \frac{\Phi}{\Phi_0}\right)$

Energy spectrum

A 1D ballistic loop:

$$\varepsilon_n = \frac{h^2}{2mL^2}\left(n + \frac{\Phi}{\Phi_0}\right)^2$$

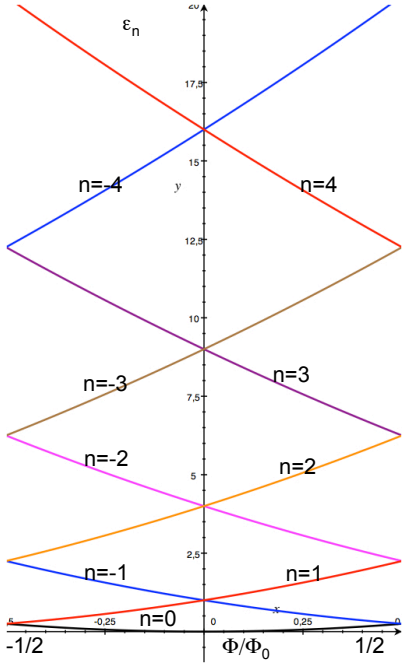

Persistent currents

For every energy level we can define an electron velocity: $v_n = \frac{1}{\hbar}\frac{\partial\varepsilon_n}{\partial k} = \frac{L}{e}\frac{\partial\varepsilon_n}{\partial\phi}$

This gives a current for every occupied state: $i_n = -\frac{ev_n}{L} = -\frac{\partial\varepsilon_n}{\partial\phi}$

The total current is the sum of the contributions of all occupied states. At T=0:

$$I_N = \sum_{n=0}^{N} i_n = -\sum_{n=0}^{N}\frac{\partial\varepsilon_n}{\partial\phi}$$

Successive states carry an opposite current.

The order of magnitude of the circulating current is given by the last level.

$$I_0 = \frac{ev_F}{L}$$

This current is **non-dissipative** as it is related to the fundamental state.

Persistent current observation

Measurement of the persistent current in a single loop, of about 1 nA.

SQUID gradiometer: two loops in series with opposite direction, only the field difference is measured.

D. Mailly et al, Phys. Rev. Lett. 70, 2020 (1993).

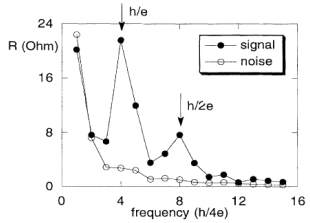

FIG. 2. Square root of spectrum power of the resistance fluctuations of the ring (mean resistance $\approx 1\ k\Omega$). Open circles correspond to experimental noise, i.e., differences between measurements with ring open. Solid circles correspond to experimental signal, i.e., differences between measurements with ring closed and ring open. The two arrows indicate the position of period h/e and $h/2e$.

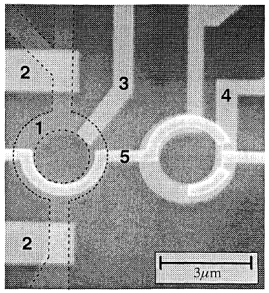

FIG. 1. Electron micrograph of the experimental device. On the left is the ring etched in GaAs 2DEG (labeled 1) (the dashed line has been added because of the poor contrast) with the two gates, (2) and (3). On the right is the calibration coil (4). On the top is the first level of the SQUID fabrication (5) with the two microbridge junctions on the right. The picture has been taken before the second level of the SQUID fabrication.

Basic definitions

Current fluctuation: $\delta I(t) = I(t) - \bar{I}$

The auto-correlation function is: $\psi(t,\tau) = \langle \delta I(t)\delta I(t+\tau)\rangle$

In the stationary case, the spectral density of the current noise:

$$S_I(f) = 2\int_{-\infty}^{\infty} \exp[2i\pi f\tau]\psi(\tau)d\tau = 2\psi(f)$$

The variance is: $\left\langle (\delta I)^2 \right\rangle = \psi(\tau = 0) = \frac{1}{2}\int_{-\infty}^{\infty} S_I(f)df = \int_0^{\infty} S_I(f)df$

Last equality true when $S_I(f) = S_I(-f)$, i.e. vacuum fluctuations are negligible.

Chapter 4:
Noise in mesoscopic systems

"The noise is the signal", Rolf Landauer, Nature 392, 658 (1998).

3.1: Thermal noise

Nyquist noise

Consider two conductors connected through a transmission line of length L.

A conductor = a pure resistor + a noise voltage source

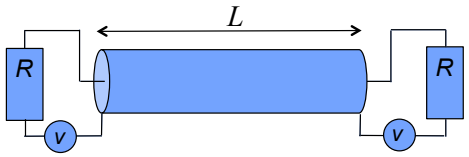

A equal power is exchanged between them: $\overline{v^2}/4R$

The noise delivered in a frequency interval $\frac{d\omega}{2\pi}$ is: $dP = \frac{1}{4R} S_V(\omega) \frac{d\omega}{2\pi}$

It takes a time L/c for a photon to travel through the line.

The energy density is then: $dE = dP.t.2 = \frac{L}{2Rc} S_V(\omega) \frac{d\omega}{2\pi}$

Nyquist noise

The line is occupied by photon modes $f_n = nc/2L$.

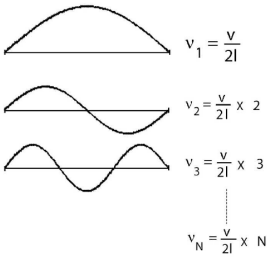

The number of modes in the frequency interval $\frac{d\omega}{2\pi}$ is:

$$m = \frac{d\omega}{2\pi} \Big/ \frac{c}{2L} = \frac{d\omega . L}{\pi c}$$

The mode occupancy is determined by the Bose-Einstein distribution function:

$$f(\omega) = \frac{1}{\exp\left(\hbar\omega / k_B T\right) - 1}$$

The energy density is then:

$$dE = \frac{L}{\pi c} \frac{\hbar\omega}{\exp\left(\hbar\omega / k_B T\right) - 1} d\omega$$

By comparing with the previous result $dE = \frac{L}{2Rc} S_V(\omega) \frac{d\omega}{2\pi}$ one obtains:

Nyquist noise

Noise density (in log scale):

$$S_V(\omega) = 4R \frac{\hbar\omega}{\exp\left(\hbar\omega / k_B T\right) - 1}$$

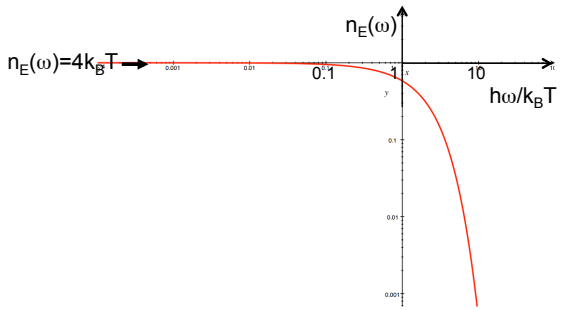

Thermal cut-off at $h\omega/k_BT$

At low frequency, one recovers the Johnson-Nyquist power density:

$S_V(\omega) = 4Rk_BT$ in V^2/Hz

The current noise is: $S_I = 4k_BT/R$ in A^2/Hz

Gives a practical voltage or current noise in $V/\sqrt{Hz}$ or $A/\sqrt{Hz}$

3.2: Shot noise

Shot noise

= bruit de grenaille = bruit de Schottky.

Basic example of the vacuum diode.

Electrons are emitted from filament to anode randomly.

The probability is constant = I/e, and $I = \frac{Ne}{\Delta t}$

Emission follows Poisson statistics (no correlation between emission times):

$$\mathrm{var}(N) = \bar{N} \qquad \mathrm{var}(I) = \mathrm{var}(N)\frac{e^2}{\Delta t^2} = \bar{N}\frac{e^2}{\Delta t^2} = \frac{Ie}{\Delta t}$$

In terms of noise current density:

$$S_I(f) = e\bar{I}$$

Usually a factor 2 appears if only positive frequencies are considered.

Measuring the shot noise is way to measure the charge of the carriers!

3.3: The tunnel junction limit

Measuring the charge of carriers: experiment

Charge is carried by 2e units at a N-S interface, due to Andreev reflection.

Noise measured is shot noise + thermal noise (visible at low bias).

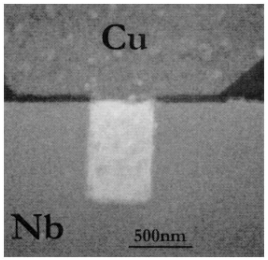

X. Jehl et al, Nature 405, 50 (2000).

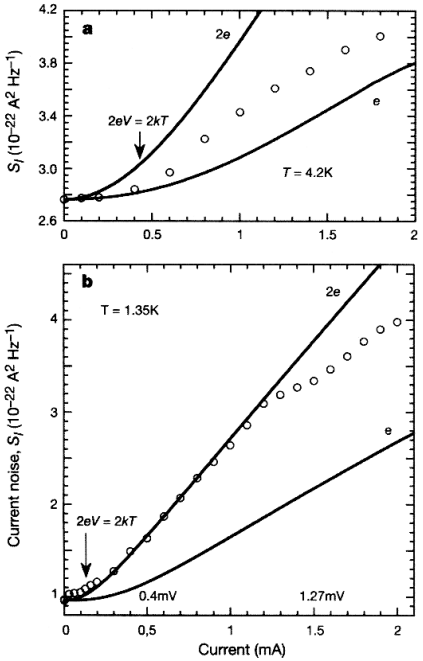

The tunnel junction limit

Let us consider the tunnel junction case. The net current writes:

$$I = \frac{4\pi e}{\hbar}\int_{-\infty}^{+\infty}|M|^2 N_A(E-eV)N_B(E)\left[f(E)\{1-f(E-eV)\} - f(E-eV)\{1-f(E)\}\right]dE$$

The current includes a subtraction between direct current and counter-current.

In the noise, both currents contribute as 2eI. The contributions are added:

$$S_I(f=0) = \frac{8\pi e^2}{\hbar}\int_{-\infty}^{+\infty}|M|^2 N_A(E-eV)N_B(E)\left[f(E)\{1-f(E-eV)\} + f(E-eV)\{1-f(E)\}\right]dE$$

We can show that: $$S_I(V) = 2e\frac{\exp\left(\frac{eV}{k_BT}\right)+1}{\exp\left(\frac{eV}{k_BT}\right)-1}I(V) = 2eI(V)\coth\left(\frac{eV}{2k_BT}\right)$$

$$f(E)\{1-f(E-eV)\} \pm f(E-eV)\{1-f(E)\}$$

$$= \frac{1}{1+\exp\left(\frac{E}{k_BT}\right)}\left\{1-\frac{1}{1+\exp\left(\frac{E-eV}{k_BT}\right)}\right\} \pm \frac{1}{1+\exp\left(\frac{E-eV}{k_BT}\right)}\left\{1-\frac{1}{1+\exp\left(\frac{E}{k_BT}\right)}\right\}$$

$$= \frac{1}{1+\exp\left(\frac{E}{k_BT}\right)}\frac{1}{1+\exp\left(\frac{E-eV}{k_BT}\right)}\left[\exp\left(\frac{E+eV}{k_BT}\right) \pm \exp\left(\frac{E}{k_BT}\right)\right]$$

$$= \frac{\exp\left(\frac{E}{k_BT}\right)}{\left[1+\exp\left(\frac{E}{k_BT}\right)\right]\left[1+\exp\left(\frac{E-eV}{k_BT}\right)\right]}\left[\exp\left(\frac{eV}{k_BT}\right) \pm 1\right]$$

$$\frac{f(E)\{1-f(E-eV)\}+f(E-eV)\{1-f(E)\}}{f(E)\{1-f(E-eV)\}-f(E-eV)\{1-f(E)\}} = \frac{\exp\left(\frac{eV}{k_BT}\right)+1}{\exp\left(\frac{eV}{k_BT}\right)-1}$$

D. Rogovin, D. Scalapino, Annals of Physics 86, 1 (1974).

The tunnel junction limit

Let us consider a ohmic resistance: $S_I(V) = 2eI.\coth\left(\frac{eV}{2k_BT}\right)$

In the limit of a zero bias, one recovers the Johnson-Nyquist noise:

$$S_I(V) = 2eI\frac{1}{\frac{eV}{2k_BT}} = 4k_BT/R$$

In the limit of a large bias, one obtains the shot noise:

$$S_I(V) = 2eI$$

A primary electronic thermometer based on shot noise measurement

Crossover between shot noise and thermal noise.

L. Spietz et al, Science 300, 1929 (2003).

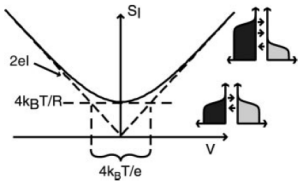

Fig. 1. Theoretical plot of current spectral density of a tunnel junction (Eq. 3) as a function of dc bias voltage. The diagonal dashed lines indicate the shot noise limit, and the horizontal dashed line indicates the Johnson noise limit. The voltage span of the intersection of these limits is $4k_BT/e$ and is indicated by vertical dashed lines. The bottom inset depicts the occupancies of the states in the electrodes in the equilibrium case, and the top inset depicts the out-of-equilibrium case where $eV \gg k_BT$.

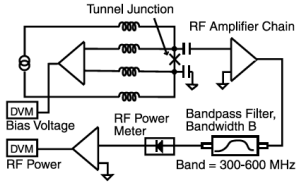

Fig. 2. Apparatus used for measurement of junction noise. Inductively coupled leads block high frequencies and allow the junction to be current-biased with one pair of leads, whereas the voltage is measured with the other pair of leads. Capacitively coupled leads allow the noise to be measured simultaneously. The noise signal is amplified by a cryogenic high electron mobility transistor amplifier and a chain of rf amplifiers, which provide about 70 dB of gain and a noise temperature of 10 K. The output of this chain is measured by a Schottky diode, which converts noise power to a dc voltage. Voltages are read out on digital volt meters (DVMs).

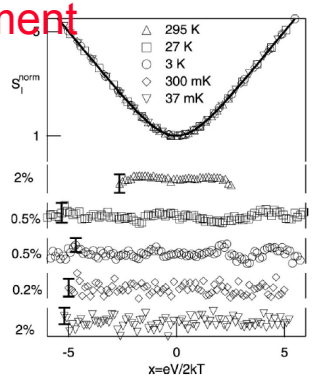

Fig. 3. Normalized junction noise plotted versus normalized voltage at various temperatures. Noise power is normalized to the zero bias (Johnson) noise, and bias voltage is scaled relative to temperature. In these units, the data follow the universal function $x\coth(x)$, depicted by the solid line. The residuals have the indicated fractional standard deviations and are shown below. This plot shows that the "gas law" for the junction noise is obeyed over four decades in temperature, with a significant systematic effect at the room temperature. Error bars indicate stated approximate SD of residuals.

3.2: Partition noise

Partition noise

I_0 particules are emitted by the reservoir during a time unit.

Probability T to have a particule transmitted.

The probability to have I particules through writes: $P_{I_0}(I) = C_I^{I_0} T^I (1-T)^{I_0-I}$

The mean current is: $\bar{I} = \sum_{I_0} P(I_0) \sum_I P_{I_0}(I) I = \sum_{I_0} P(I_0) T I_0 = T\bar{I_0}$ seems actually obvious

Here we have used: $(a+b)^n = \sum_p C_p^n a^p b^{n-p}$

$$\frac{d}{da}(a+b)^n = n(a+b)^{n-1} = \sum_p p C_p^n a^{p-1} b^{n-p} = \frac{1}{a}\sum_p p C_p^n a^p b^{n-p}$$

with a = T, b = 1 – T and n = I_0.

$$I_0 (1)^{I_0-1} = I_0 = \frac{1}{T}\sum_{I_0} C_I^{I_0} T^I (1-T)^{I_0-I} I = \frac{1}{T}\sum_{I_0} P_{I_0}(I) I$$

Partition noise

We consider the noise: $\overline{\Delta I^2} = \overline{I^2} - \bar{I}^2$

Let's calculate the mean of I^2: $\overline{I^2} = \sum_{I_0} P(I_0) \sum_I P_{I_0}(I) I^2$

Same trick:

$$\frac{d^2}{da^2}(a+b)^n = n(n-1)(a+b)^{n-2} = \sum_p p(p-1) C_p^n a^{p-2} b^{n-p}$$

$$I_0(I_0-1) = \frac{1}{T^2}\left[\overline{I^2} - \bar{I}\right] \Rightarrow \overline{I^2} = T^2 I_0^2 + T I_0 (1-T)$$

$$\overline{I^2} = \sum_{I_0} P(I_0) \sum_I I^2 P_{I_0}(I) = \sum_{I_0} P(I_0)\left[T^2 I_0^2 + I_0 T(1-T)\right]$$

$$\overline{\Delta I^2} = T^2 \sum_{I_0} P(I_0) I_0^2 + T(1-T)\sum_{I_0} P(I_0) I_0 - T^2 \bar{I_0}^2 = T^2\left[\overline{I_0^2} - \bar{I_0}^2\right] + T(1-T)\bar{I_0}$$

Partition noise

We obtained the shot noise of a single conductance channel:

$$\overline{\Delta I^2} = T^2 \overline{\Delta I_0^2} + T(1-T)\bar{I_0}$$

Noise of the source transmitted by the channel

Partition noise

Charge e not included here

Assume a noise-free emitter: $\overline{\Delta I^2} = T(1-T)\bar{I_0} = (1-T)\bar{I}$

In the limit T small, one recovers the shot noise: $\overline{\Delta I^2} \propto \bar{I}$

In the case of multiple channels: $\overline{\Delta I^2} = \sum_p T_p (1-T_p)\bar{I_0}$

The reduction factor is the Fano factor: $F = \frac{\overline{\Delta I^2}}{\bar{I}} = \frac{\sum_p T_p(1-T_p)\bar{I_0}}{\sum_p T_p \bar{I_0}}$

Partition noise: experiment

A. Kumar, et al, Phys. Rev. Lett. 76, 2778 (1996).

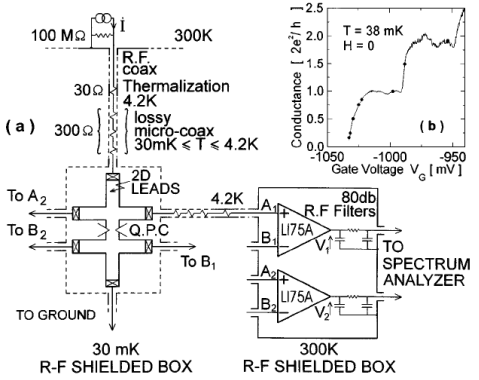

FIG. 1. (a) Schematic measurement circuit. (b) QPC conductance vs gate voltage for $H = 0$. The black points show the values of G and gate voltage where noise is studied.

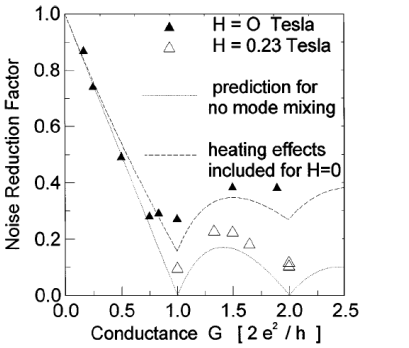

FIG. 4. Noise reduction factor vs the conductance for $H = 0$ (filled triangles) and $H = 0.23$ T (open triangles). Predictions for no mode mixing without (dotted curve) and with (dashed curve) the calculable heating effects for $H = 0$.